Journal of Intelligent & Fuzzy Systems 28 (2015) 2605–2620
DOI:10.3233/IFS-151539
IOS Press

Fuzzy fault tolerant control for smart lights

Jose J. Velasquez and Kevin M. Passino*
Department of Electrical and Computer Engineering, Ohio State University, Columbus, OH, USA

Abstract. This paper investigates the implementation of adaptive and nonadaptive fuzzy controls for a smart lights experimental testbed. The objective is to accurately regulate the light level across the experimental testbed to a desired value, and to test the performance of the fuzzy controllers under cross-illumination effects and bulb and sensor failures. As an initial approach, a decentralized (i.e., no communication between controllers) nonadaptive fuzzy controller is implemented and applied to the smart lights. This approach is convenient for this type of experimental testbed where a mathematical model of the plant is not available and heuristic information about how to control the system is sufficient. The nonadaptive fuzzy controller, when properly tuned, is able to achieve uniform lighting across the entire testbed floor in most of the tested situations but it fails whenever an on/off light bulb failure is introduced. In order to attain uniform lighting in the presence of failures, a "fuzzy model reference learning controller" (i.e., adaptive fuzzy controller) is implemented for the smart lights, and this algorithm proves to be able to successfully adapt to uncertainties such as disturbances and failures.

Keywords: Adaptive algorithm, adaptive fuzzy control, lighting control, fuzzy control

1. Introduction

Lighting represents one of the key components of today's residential and commercial buildings. In fact, lighting consumes around 35% of the electricity used in commercial buildings in the United States. Also, lighting uses 18% of the electricity produced in the U.S., and an additional 4% to 5% has to be used just to remove the waste heat caused by the lights [19]. A good smart lighting system can be a promising solution to this energy consumption problem. The lighting energy use in most buildings can be reduced significantly while maintaining the quality of service. This reduction of electricity use can be achieved by reducing the over-illumination produced by neighboring lights and considering external light sources (e.g., daylight harvesting). A significant saving (up to 40%) can be obtained by applying modern control strategies such as daylight harvesting, occupancy sensing, scheduling, and load shedding [9, 10].

Over the last several years, in order to improve the lighting use in commercial buildings and reduce the utility costs, smart lighting systems have been developed and implemented for controlling the illumination level in an office setting [4, 9, 20, 21]. Martirano discusses the importance of using efficiency and effectiveness to approach a smart lighting control problem [9]. Efficiency is achieved via using low consumption equipment (i.e., LED luminaries) and improved lighting design practices (i.e., localized task lighting systems). Effectiveness is achieved by improving the current lighting control systems to avoid additional unnecessary energy use and adopting a technical building management system (i.e., maintenance and metering). This research claims that a smart lighting control system can result in saving up to 25% in industrial and commercial buildings, and up to 45% in tertiary and educational buildings [9].

*Corresponding author. Kevin M. Passino, Department of Electrical and Computer Engineering, Ohio State University, Columbus, OH 43210, USA. Tel.: +1 614 312 2472; E-mail: passino.1@osu.edu.

Wen et al. developed an energy-efficient lighting system based on wireless sensor network technology [20, 21]. In this system, they implemented a centralized intelligent lighting optimization algorithm where the overall lighting in an office is determined as a linear combination of the light contributions from each of the luminaries based on a discretization of the office into square grids. This light setting control is coded as a linear programming optimization problem supported by the fact that the power consumption is directly proportional to the light output from the luminaries, and hence, minimizing the illuminances is similar to minimizing the electricity usage. Once the centralized optimization algorithm computes the optimal linear combination of the individual luminaries that minimizes the entire lighting output, then the control signal is sent via the wireless network [20, 21].

An adaptive lighting system has been developed in [4]. Hughes et al. proposed the use of an intelligent control system that allows the lighting system to dynamically respond to the current conditions of the area it illuminates. For this adaptive system, they have included within their control loop occupancy sensors, photosensors, and personal control modules. The proposed adaptive lighting system is programmed to maintain the desired ambient illumination levels and continuously adjust task illumination levels in individual areas as occupancy varies. This adaptive control system has been able to provide a significant reduction in energy consumption of about 69% compared to a conventional static lighting system [4].

There has been significant work on the development of stable fuzzy/neural adaptive controllers [17, 18], even for multi-input multi-output (MIMO) systems [11]; however, the smart lights testbed does not fit the mathematical assumptions in those papers needed to guarantee stability. First, an individual isolated zone acts like a first order system with a delay making the system infinite dimensional so that none of the existing theory applies. Moreover, our plant has eight inputs and eight outputs and is highly coupled, and not coupled in a way that the "diagonal dominance" conditions in [11] are met, and hence stability cannot be guaranteed. Due to the lack of a mathematical model of the plant and lack of existing control theory for coupled MIMO systems with a delay, a control strategy where heuristic information about how to control the system is required. Heuristic based control strategies include neural networks, fuzzy control, adaptive neural/fuzzy control, genetic algorithms for adaptive control, etc. Here, we select a nonadaptive and adaptive fuzzy control as candidate control strategies for our smart lights testbed.

In relation to fault-tolerant control, most researchers view faults as structural or parameter changes and then use some type of robust control (e.g., sliding mode control or adaptive control) to reduce the effect of the changes. Here, we use adaptive fuzzy control since it has been shown [18] that it can cope with large and nonlinear changes in a plant. Unlike in [6], there is no need for other fault tolerant control strategies beyond this adaptive strategy (e.g., a fault diagnosis strategy coupled with a control-redesign strategy). There have been several studies on how to achieve fault tolerant control via adaptive fuzzy/neural control. An intelligent fault-tolerant control system is developed in [1]. Diao et al. proposed a design model of a turbine engine system using a hierarchical learning structure in the form of Takagi-Sugeno fuzzy systems. For this fault-tolerant control approach, the control scheme is designed based on stable adaptive fuzzy/neural control where the on-line learning capabilities of the controller capture the unknown dynamics caused by the failures. A novel fault-tolerant control methodology using adaptive estimation and control approaches based on the learning capabilities of neural networks or fuzzy systems is described in [2]. For this methodology, an on-line approximation-based stable adaptive neural/fuzzy control is considered for a class of input-output feedback linearizable time-varying nonlinear systems. Stable indirect and direct adaptive controllers are discussed for a class of input-output feedback linearizable time-varying non-linear systems in [3]. These indirect and direct adaptive controllers present stable performance for a fault-tolerant engine control problem.

This paper provides the first application of fuzzy control to intelligent illumination control. The implemented adaptive fuzzy controller has been able to effectively achieve uniform lighting across the entire floor of the experimental testbed under different testbed settings. The "no-partition case" has been the selected to present most of our experimental results since it represents the most challenging illumination control problem (since it provides maximized cross-illumination between zones). We have proposed a decentralized control approach where each zone of the testbed has an independent fuzzy controller (unlike in [5]). This eliminates the need for communication between the zones, and furthermore, we do not need a sensor network (as they do in [20, 21]) to acquire the data, compute the control action, and then apply the control signal to the plant. Our approach achieves

significantly better results than other approaches such as the conventional decentralized integral controls and the illumination balancing algorithm (IBA) in [5]. The improvements compared to previous work (i.e., like [5]) include: first, a faster transient response which means faster rise time and settling time to achieve the desired light level which is a desired feature in a lighting system, and second, improved uniform lighting under maximized cross-illumination effects (i.e., "no-partition case") something that the decentralized integral control failed to do and for which the IBA showed poor tracking performance as illustrated in [5].

In this paper, we adapted the "fuzzy model reference learning controller" (FMRLC) approach [7, 8] to our smart lighting testbed, something that has not been done before. Here, we have demonstrated the following advantages of the FMRLC: improved convergence rates (i.e., faster transient response), use of less control energy (i.e., reduced light consumption) by applying lower voltage levels to the light bulbs compared to the fuzzy controller, decentralized integral control, and IBA in most of the presented cases, enhanced disturbance rejection properties (i.e., rejection of light bulb and sensor failures), and lack of dependence on a mathematical model (i.e., heuristic knowledge about the plant is sufficient). All these facts are supported by experimental results obtained from the testbed. This is the first study of fault tolerant control for smart light systems.

2. Experimental testbed

2.1. Testbed layout

The experimental testbed is made up from a box of $22.5 \times 33 \times 12$ cm. The floor plan of the testbed is presented in Fig. 1. Notice that the eight zones are not equally distributed across the entire floorplan. Zones 1 and 2 are 11.25×10 cm, zones 3 and 4 are 11.25×6.5 cm, zones 5 and 6 are 11.25×7.5 cm, and zones 7 and 8 are 11.25×9 cm.

The bold lines separating each zone represent cardboard "partitions" that can be set up between the zones in order to simulate partition in an office building. There are three main room partition settings: full height, half height, and no partition. Full height partitions provide the case where there are eight independent rooms (i.e., eight independent sensors), half height partitions gives us the case with some cross-illumination effect between neighboring rooms (like a typical office building), and the case of no partitions introduces maximized cross-

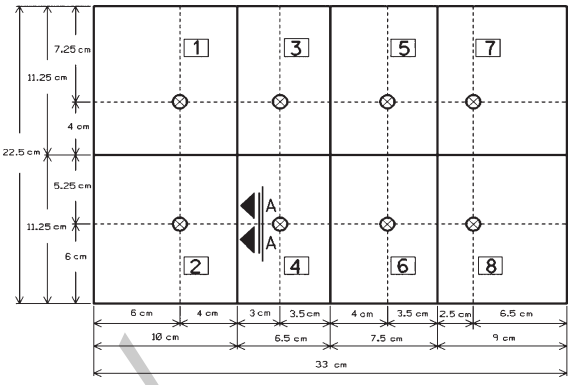

Fig. 1. Floor plan of the experimental testbed for smart lights.

illumination effects through out the entire testbed (the situation for large open areas in a room). In this paper, to avoid introducing too many plots, we will focus in the no partition case because it provides the most challenging control problem as described in [5, 14, 15], but we also discuss the sensor failure case. However, all the control algorithms were tested under all the room settings to guarantee a stable system performance.

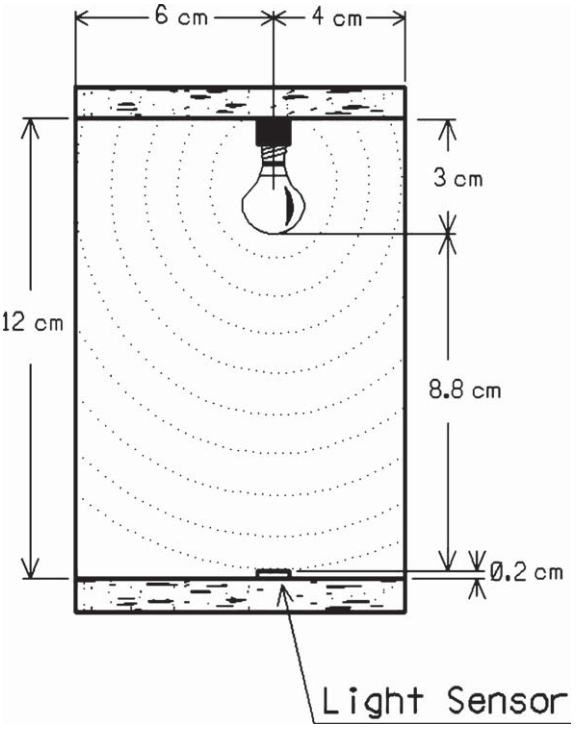

Fig. 2. Cross section view "AA" of zone 2 illustrating light bulb and sensor.

The cross section view "AA" of zone 2 (see Fig. 1) illustrating the location of both the light bulb and the light sensor is presented in Fig. 2. Notice that the light bulb is located right above the light sensor for better light sensing. The light bulb is a miniature incandescent bulb (base #1847) of 0.25 Watts operating at 6.3 Volts with a length of 3 cm. The light sensor is a Cadmium-Sulfide (CdS) photocell (RadioSchack Part #276-1657) featuring visible light response, sintered construction, and low cost [16].

2.2. Driving and acquisition circuitry

The smart lighting experimental testbed has both driving and acquisition circuitry. These two main circuitries are interfaced by means of a research and development (R&D) controller board from dSPACE Inc. The dSPACE DS1104 R&D controller board is equipped with real-time interface (RTI) which can be graphically programmed in Simulink from MATLAB. The DS1104 board provides us with eight analog to digital converter (ADC) channels to interface the output of the light sensors with the controller coded in the digital computer and eight digital to analog converter (DAC) channels to interface the controller output to the light bulbs as an analog signal.

The schematic layout for the driving circuits in each zone of the testbed is given in Fig. 3. The driving circuitry is intended to provide the necessary current for the light bulbs in each corresponding zone by using a power transistor as a common-collector amplifier (i.e., a voltage buffer). As illustrated in Fig. 3, each zone of the experimental testbed has its independent driving circuit.

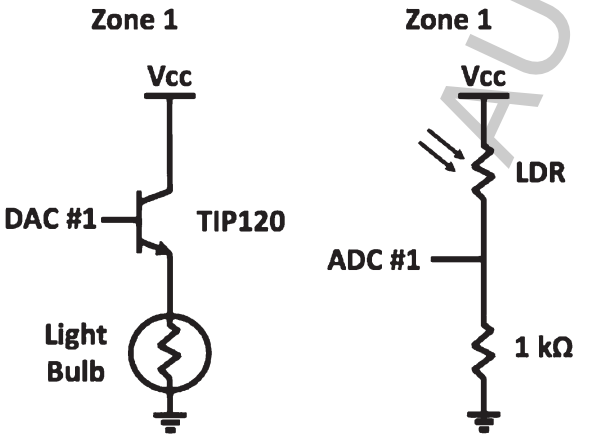

Fig. 3. Left: Driving circuitry for each zone of the experimental testbed is in the same form as the one shown above for zone 1. Right: Acquisition circuitry for each zone of the experimental testbed is in the same form as the one shown above for zone 1.

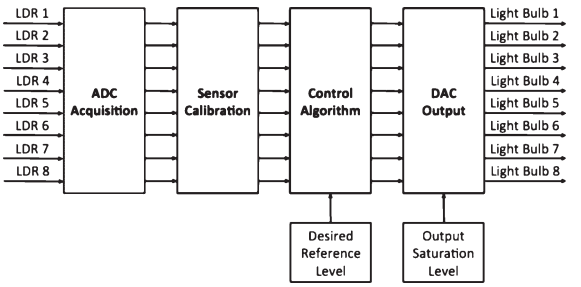

Fig. 4. Overall control loop diagram.

The schematic layout for the acquisition circuits in each zone of the testbed is shown Fig. 3. The acquisition circuitry is designed to provide a voltage signal (i.e., an analog signal) to each one of the analog to digital converter channels. As shown in Fig. 3, each zone of the testbed has its independent acquisition circuit. A light dependent resistor (LDR) is used to measure the illuminance of the light bulbs over the testbed floor in Volts since this is proportional to measuring illumination in lux (i.e., lux = constant × Volt). The proportionality constant depends on the resistance vs. illumination characteristics of the LDR. The acquisition circuitry is formed by a voltage divider which basically will output as much as the source voltage (i.e., $V_{cc} = 13.4$ V) as the illumination on the LDR increases, or a smaller voltage (i.e., tending to zero) as the illumination on the LDR decreases.

2.3. Overall control loop

The overall control loop diagram implemented for our smart lighting system is illustrated in Fig. 4. The control loop is composed of four main parts: ADC acquisition, sensor calibration, control algorithm, and DAC output. Each part of the control loop plays a key role in our system and both the ADC acquisition and DAC output let us create the interface between the digital and analog world. Both the sensor calibration and the control algorithms are coded into the digital computer.

3. Fuzzy control for smart lights

Fuzzy control has become an alternative to classical control schemes because the controller design does not depend on a mathematical model but on the knowledge

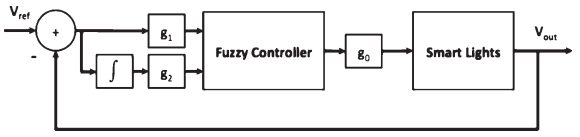

Fig. 5. PI fuzzy controller for smart lights with scaling gains.

that the control engineer has about how to accurately control the plant. In this section, we will present the implementation details related to our fuzzy and adaptive fuzzy controller. For the reader interested in the details for the design of a fuzzy and adaptive fuzzy controller, we encourage to review the description developed in [7, 8, 12, 13].

3.1. Design case: Direct PI fuzzy control for smart lights

For our smart lighting system, we have the selected the inputs of the fuzzy controller as the "error" ($e(t)$) and "integral-of-error" ($\int e(t)dt$), and the output as the "applied voltage" ($V_{app}(t)$). We implemented 11 uniformly space triangular membership functions for each controller input. Our designed fuzzy controller was tested directly on the plant and then we proceeded to adjust the controller gain during implementation.

The fuzzy controller implemented in our experimental testbed is illustrated in Fig. 5. Notice from Fig. 5 that we have added the gains g_1 and g_2 at the inputs and g_0 at the output of the fuzzy controller. These gains have been added because they are useful in tuning the fuzzy controller. The gains can scale the horizontal input and output axes of the fuzzy controller. In our implementation, we "normalized" [13] the input and output universe of discourse.

The scaling gains play an important key role in the performance of the fuzzy controller. Notice that the scaling gain g_1 in the input is equivalent to scaling the horizontal axis of the $e(t)$ universe of discourse by $1/g_1$. The scaling g_1 will introduce the following effects:

1. If $g_1 = 1$, the membership functions are not changed, therefore there is no change on the meaning of the linguistic values.
2. If $g_1 < 1$, the membership functions are uniformly "spread out" by a factor of $1/g_1$.
3. If $g_1 > 1$, the membership functions are uniformly "contracted."

Similarly, the scaling gain g_2 will have the same effects for the $\int e(t)dt$ universe of discourse. For the

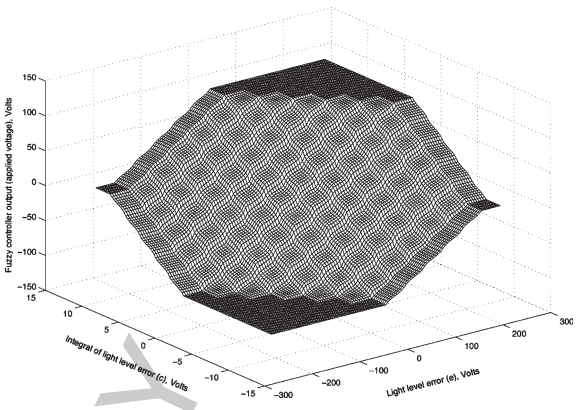

Fig. 6. Nonlinear control surface by PI fuzzy controller for smart lights.

output universe of discourse, the scaling gain g_0 is a multiplying factor to the horizontal $V_{app}(t)$ axis. For our smart light system, we found after several trials and errors that the scaling gains $g_1 = 0.005$, $g_2 = 0.10$, and $g_0 = 100$ provide the best tuned performance. Generally speaking, the gains g_1, g_2 and g_0 are used to normalize the universe of discourse for the error $e(kT)$, integral-of-error $c(kT)$, and controller output $u(kT)$, respectively. The gain g_1 is selected so that the range of values of $g_1 e(kT)$ lie on $[-1, 1]$ and g_0 is selected by taking into consideration the valid range of inputs to the plant using a similar approach. The gain g_2 is determined by looking at the normal range of values that $c(kT)$ will take for a different set of inputs to the system. Hence, the gain g_2 is selected so that $g_2 c(kT)$ range of values are scaled to $[-1, 1]$. The scaling gains g_1, g_2 and g_0 are tuned following the design procedure discussed in [7, 8, 13].

One of the most important characteristics of a fuzzy controller compared to a linear controller is its control surface. Fuzzy controllers can generate a nonlinear control surface which is desired for some control applications. The nonlinear control surface implemented by the PI fuzzy controller is shown in Fig. 6. This control surface provides another way to view the user expertise on how to control the output voltage (i.e., room illumination).

3.2. Design case: FMRLC for smart lights

The block diagram of the FMRLC is presented in Fig. 7. Notice from Fig. 7 that the FMRLC has four main components: the plant, the fuzzy controller to be tuned, the reference model, and the learning (i.e, adaptation) mechanism.

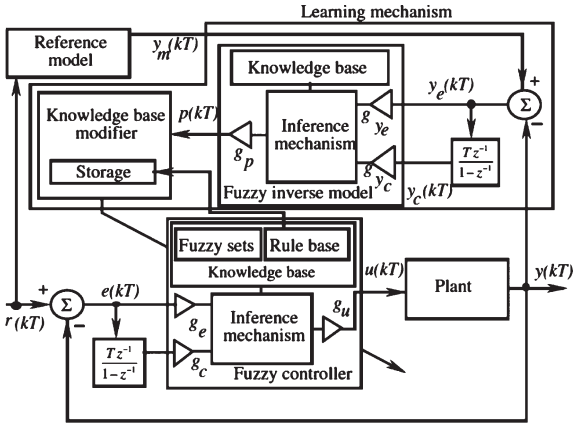

Fig. 7. Fuzzy model reference learning controller (adapted from [8]).

The FMRLC observes the data from the fuzzy control system, which means the reference input $r(kT)$ and the plant output $y(kT)$ where T is the sampling period of the digital computer. From the measured numerical data, the FMLRC considers the fuzzy control system's current performance and automatically adjusts (i.e., tunes) the fuzzy controller so that the closed-loop system (mapping from $r(kT)$ to $y(kT)$) behaves like the given reference model (mapping $r(kT)$ to $y_m(kT)$). In general, the fuzzy controller loop (the bottom of Fig. 7) makes $y(kT)$ track $r(kT)$ by adjusting $u(kT)$ and the learning control loop (the top of Fig. 7) makes the output of the plant $y(kT)$ track the output of the reference model $y_m(kT)$ by tuning the fuzzy controller parameters. A new notation is introduced to provide a more intuitive explanation of the FMRLC components in terms of light voltage levels and present the FMRLC block diagram without significant modifications from the original in [8]. Notice that the notations V_{ref}, $V_{out}(kT)$, $V_m(kT)$, $V_e(kT)$, and $V_c(kT)$ respectively represent the notations $r(kT)$, $y(kT)$, $y_m(kT)$, $y_e(kT)$ and $y_c(kT)$ in Fig. 7.

For the fuzzy controller in Fig. 7, we selected $e(kT) = V_{ref}(kT) - V_{out}(kT)$ and $c(kT) = c(kT - T) + Te(kT - T)$ as the inputs, where $V_{ref}(kT)$ is the desired input reference voltage. We chose $T = 0.001$ seconds for our implementation in the dSPACE board. The controller output is given by the output voltage $V_{out}(kT)$ of the smart light. We implemented 11 uniformly spaced triangular membership function for each controller input (i.e, for $e(kT)$ and $c(kT)$). We selected the scaling gains for the fuzzy controller in Fig. 7 to be $g_e = 0.005$, $g_c = 0.10$, and $g_u = 100$ (i.e., the ones we tuned above) which follow the same tuning procedure as g_1, g_2 and g_0. The output membership functions were defined to be symmetric and triangular shaped with a base width of 0.4 on a normalized output universe of discourse as well. The reference model is selected to be

$$\frac{V_m(s)}{V_{ref}(s)} = \frac{\frac{1}{200}}{s + \frac{1}{200}} \tag{1}$$

where $V_m(s)$ indicates the desired system performance for the output voltage of the smart light $V_{out}(t)$. The reference model given in Equation 1 is selected based on how we would like the plant to behave, here a first order system with a very fast pole (i.e., a very fast transient response desired for a lighting system). For the fuzzy inverse model, the inputs are selected to be $V_e(kT) = V_m(kT) - V_{out}(kT)$ and $V_c(kT) = V_e(kT) + TV_e(kT - T)$. Similar to the fuzzy model, we implemented 11 fuzzy sets with symmetric and triangular shaped membership functions, which are also evenly distributed on the corresponding universes of discourse. The scaling gains for the fuzzy inverse model were selected as $g_{y_e} = 0.0005$, $g_{y_c} = 0.001$, and $g_p = 1$ respectively. These scaling gains g_{ye}, g_{yc}, and g_p are selected by following the design procedure described in detail in [7, 8].

4. Simple fault tolerance test results

The simple fault tolerance test is performed in order to study the controller's performance under a specific fault test with no partitions between zones such that a proper operation of the smart lights can be guaranteed for a commercial application. Moreover, we are more concerned with the capability of the "learning" control algorithm (i.e., FMRLC) to perform on-line adaptation of the fuzzy rule-base to overcome a system failure compared to the performance of the nonadaptive control algorithm (i.e., fuzzy controller). Implementation results for a simple fault tolerance case are separated into two main cases: single zone and multiple zones light bulb failure.

4.1. Single zone light bulb failure

When a light bulb failure (i.e., when a bulb blows out) is introduced in the experimental testbed at $t = 30$ seconds in zone 1 (i.e., upper left corner), the PI fuzzy controller is able to maintain uniform lighting in the remaining seven zones as illustrated in Fig. 8. The unit "Volt" is used to measure the light levels in Fig. 8

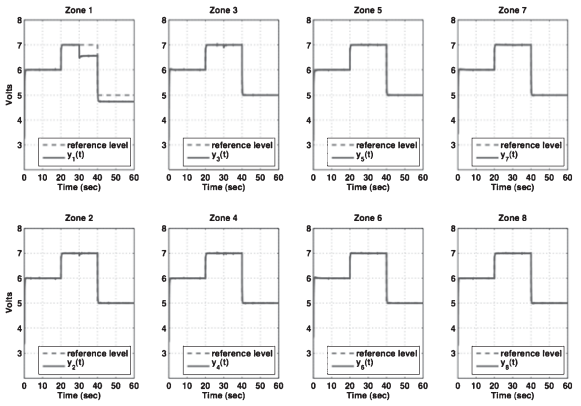

Fig. 8. Light levels at each zone for the PI fuzzy controller with no partition between zones under zone 1 light bulb failure.

because these measurements result from the voltage signals of the acquisition circuitry in Fig. 3. Clearly, the light level in zone 1 drops to a fixed value given by the cross-illumination effect imposed by the neighboring zones. Notice in Fig. 8 that very small undershoots can be seen in zones 2, 3, 4, 5, and 7 due to the presence of the failure produced in zone 1.

By looking at the applied voltage level to the light bulbs (i.e., control signal) on each zone for this particular case given in Fig. 9, we can observe how the controller reacts to the zone 1 failure after $t = 30$ seconds. Zones 2, 3, 4, 5, and 7 control signals show a significant change in the shape of the applied voltage which is connected with the presence of the undershoots mentioned above. These undershoots are not desirable but they are so small and fast that it will not even be perceptible by a human eye. Moreover, this unbalance

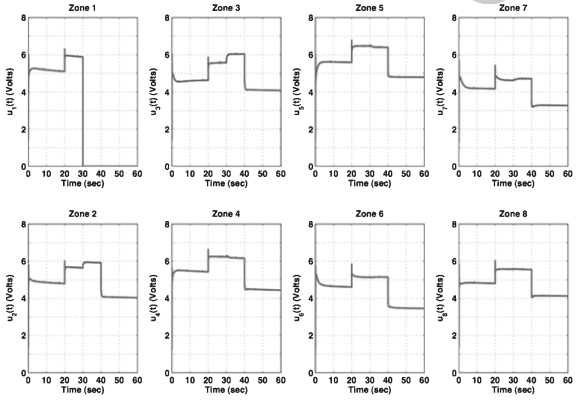

Fig. 9. Applied voltage level to the light bulbs at each zone for the PI fuzzy controller with no partition between zones under zone 1 light bulb failure.

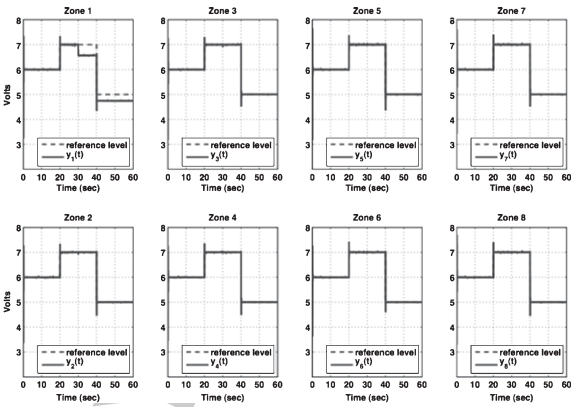

Fig. 10. Light levels at each zone for the direct adaptive PI fuzzy controller with no partition between zones under zone 1 light bulb failure.

introduced by the zone 1 failure is clearly not perturbing the light sensors in zones 6 and 8 showing the disturbance rejection of the fuzzy controller.

Next, a light bulb failure is generated in zone 1 at $t = 30$ seconds for the direct adaptive PI fuzzy controller (i.e., FMRLC). As shown in Fig. 10, this controller is able to maintain uniform lighting in the remaining seven zones. From Fig. 10, the presence of a learning control algorithm is evident. The existence of a very fast overshoot for the raising reference and a very fast undershoot for the falling reference is caused by the way the inverse fuzzy model gains are tuned. This does not mean that this is a poor performance, in fact, the adaptive fuzzy controller is tuned in such a way that it is quick to adapt to abrupt changes in the plant parameters (e.g., light bulb failures) as is presented with these experimental results.

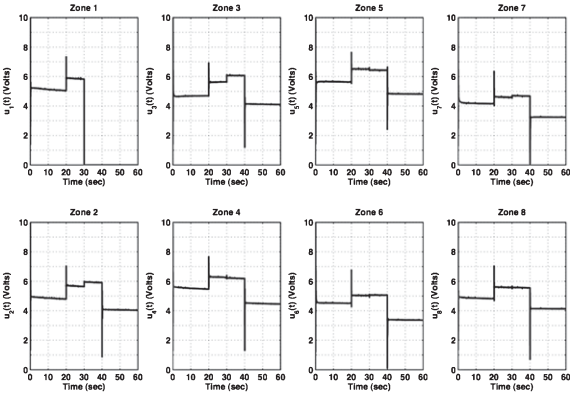

Fig. 11. Applied voltage level to the light bulbs at each zone for the direct adaptive PI fuzzy controller with no partition between zones under zone 1 light bulb failure.

The applied voltage level to the light bulbs on each zone for this particular case is given in Fig. 11. Again, the faster response of the adaptive fuzzy controller is seen as well as a better disturbance rejection. Moreover, comparing the light level results for the fuzzy controller (i.e., Fig. 8) and the direct adaptive fuzzy controller (i.e., Fig. 11), very fast undershoots of less than 0.2 seconds are only seen in the zones 2 and 3 (i.e, immediate neighboring zones of zone 1) for the adaptive fuzzy controller compared to slow undershoots of more than 0.5 seconds given in zones 2, 3, and 4 for the fuzzy controller when a light bulb failure is introduced in zone 1 (i.e., at $t = 30$ seconds). A detailed view of the failure effects will be presented for the multiple zone light bulb failure case in the following subsection for further understanding of this phenomena. This result points out that a properly tuned adaptive control algorithm is a good candidate for controlling a smart lights system.

4.2. Multiple zone light bulb failure

This failure is generated by shutting down the light bulbs (i.e., blowing them out) in four zones of the experimental testbed. For this multiple zone failure, the learning control algorithm is expected to track the desired light level in the remaining controlled zones, and shows a faster response to the system disturbance as well as a smaller undershoot.

A light bulb failure is created in zones 3, 4, 5, and 6 at $t = 30$ seconds. The PI fuzzy controller keeps track of the desired light level for this particular type of four-zone simultaneous failure as illustrated in Fig. 12. A typical reaction of the controller (i.e., undershoot at failure time) to reject the plant disturbance is observed in zones 1, 2, 7, and 8 respectively.

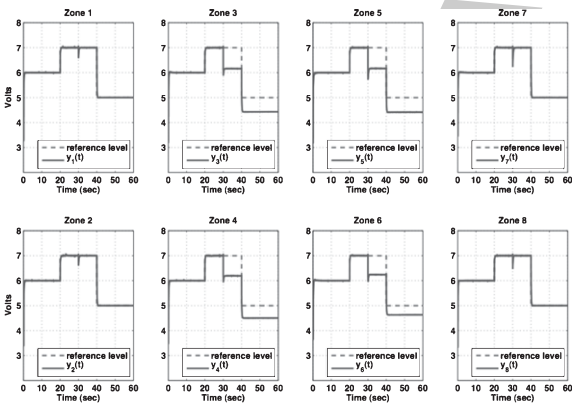

Fig. 12. Light levels at each zone for the PI fuzzy controller with no partition between zones under zones 3, 4, 5, and 6 light bulb failure.

As presented in Fig. 12, the uncontrolled zones 3, 4, 5 and 6 have a fixed light level after the failure occurs. In average, all the uncontrolled zones have the same light level between $t = 30$ seconds and $t = 40$ seconds and slightly different light levels between $t = 40$ seconds and $t = 60$ seconds because of the reduction of the desired reference level, and hence, a decrease in the cross-illumination effect due to the remaining controlled zones (i.e., zones 1, 2, 7, and 8). This is an interesting type of failure for two reasons: first, the introduced disturbance to the plant has a greater impact because the four failing zones are neighboring zones to each other, and secondly, two separated areas (i.e., zones 1-2 and zones 7-8) are created by assuming that they are far enough that there are no cross-illumination effects between them.

As given in Fig. 13, the applied voltage levels drop to zero in zones 3, 4, 5, and 6 when the failure is activated. Once the failure is active, zones 1, 2, 7, and 8 instantly increase the applied voltage level to the light bulbs so that they can compensate the failure. This fast voltage increase is reflected in the light level for the controlled zones by means of an undershoot as presented in Fig. 12 for this failure case. Moreover, a closer look at these undershoots will provide additional information on how the PI fuzzy controller is able to reject this specific disturbance. From Fig. 14, a critically damped system response is illustrated in all controlled zones. Furthermore, zone 7 exhibits the highest undershoot peak at approximately 0.75 Volts below the desired reference level and a settling time of approximately 1.2 seconds. Zone 8 shows the second highest undershoot peak at approximately 0.5 Volts below the desired light

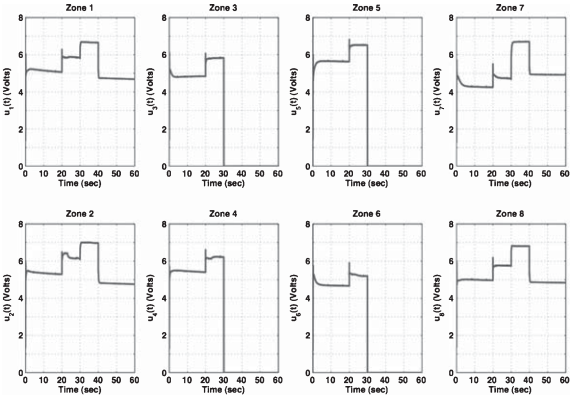

Fig. 13. Applied voltage level to the light bulbs at each zone for the PI fuzzy controller with no partition between zones under zones 3, 4, 5, and 6 light bulb failure.

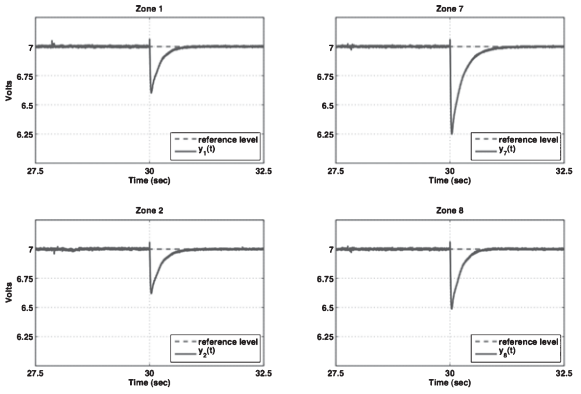

Fig. 14. Light level in controlled zones 1, 2, 7, and 8 for the PI fuzzy controller with no partition between zones under zones 3, 4, 5, and 6 light bulb failure.

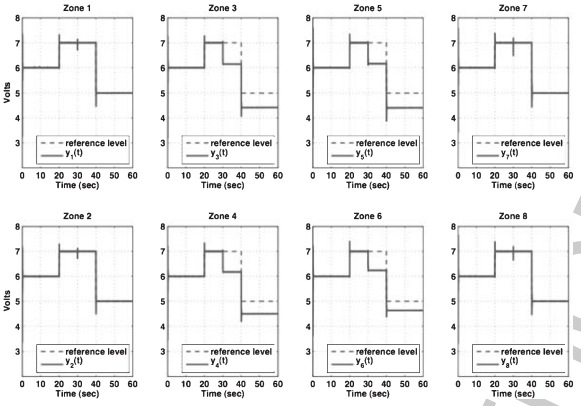

Fig. 15. Light levels at each zone for the direct adaptive PI fuzzy controller with no partition between zones under zones 3, 4, 5, and 6 light bulb failure.

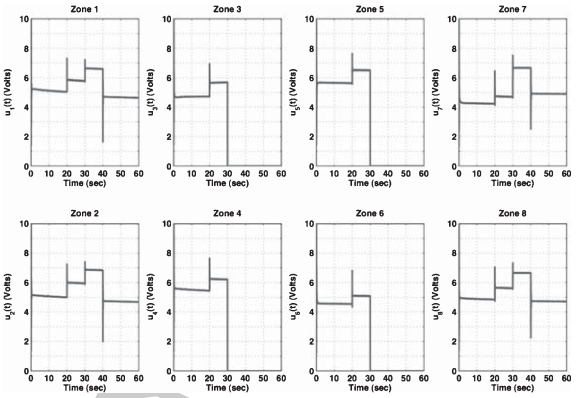

Fig. 16. Applied voltage level to the light bulbs at each zone for the direct adaptive PI fuzzy controller with no partition between zones under zones 3, 4, 5, and 6 light bulb failure.

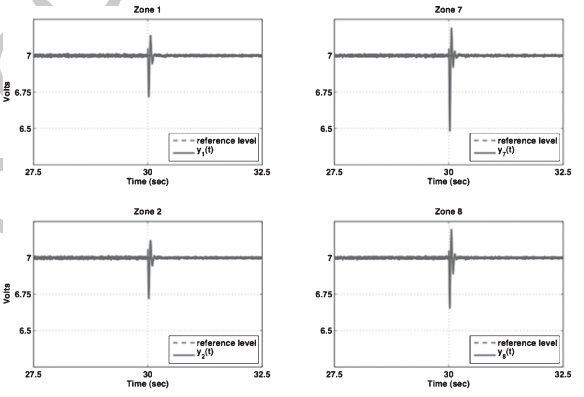

Fig. 17. Light level in controlled zones 1, 2, 7, and 8 for the direct adaptive PI fuzzy controller with no partition between zones under zones 3, 4, 5, and 6 light bulb failure.

reference level and a settling time of approximately 1 second. Zones 1 and 2 present the same undershoot peak at 0.375 Volts below the desired light reference level and a settling time of approximately 0.625 seconds.

Next, a light bulb failure is initiated in zones 3, 4, 5, and 6 at $t = 30$ seconds for the direct adaptive PI fuzzy controller. Implementation results given in Fig. 15 illustrate how the learning control algorithm keeps track of the desired light level reference after introducing a light bulb failure in four neighboring zones (i.e., increased plant disturbance effect). Notice from Fig. 15 that the fixed light level in the uncontrolled zones is comparable to the ones obtained for the nonapdative fuzzy controller. The overall system response of both controllers is very similar until we take a closer look to the disturbance rejection as illustrated in Fig. 17. The adaptive fuzzy controller exhibits very fast overshoots and undershoots whenever a change in the desired reference light level occurs in the plant but those peaks can be neglected due to very fast convergence.

As shown in Fig. 16, the applied voltage level by the adaptive control algorithm is slightly lower (a few millivolts), as compared with the nonadaptive control algorithm, for all the controlled zones (i.e, zones 1, 2, 7, and 8) given in Fig. 13.

Implementation results of the direct adaptive PI fuzzy controller during the occurrence of the light bulb failure in zones 3, 4, 5, and 6 are presented in Fig. 17. The highest undershoot peak is in zone 7 at 0.5 Volts below the desired reference level which constitutes approximately a 33.33% peak reduction compared to the nonadaptive control algorithm (i.e., Fig. 14). The highest overshoot

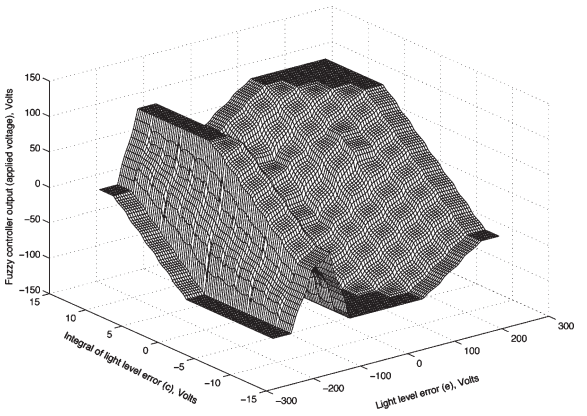

Fig. 18. Nonlinear control surface implemented by the PI fuzzy controller in zone 1 at $t = 60$ seconds under zones 3, 4, 5, and 6 light bulb failure.

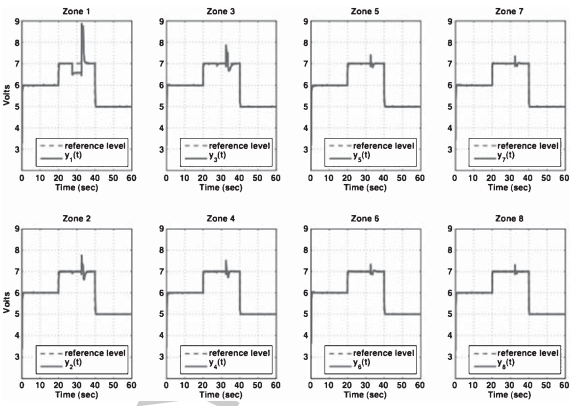

Fig. 19. Light levels at each zone for the PI fuzzy controller with no partition between zones under zone 1 on/off light bulb failure.

peak is given by zones 7 and 8 at approximately 0.187 Volts above the desired reference level. Certainly, a faster settling time of approximately 0.15 seconds is observed from all the controlled zones as compared to the PI fuzzy controller that represents a 70% reduction in settling time compared with the faster settling time zones given in Fig. 14 (i.e., zones 1 and 2).

The ability of the fuzzy controller to achieve a nonlinear control surface is seen in Fig. 6. In order to show the learning capacity of the FMRLC, we present the nonlinear control surface achieved when a light bulb failure is introduced in zones 3, 4, 5, and 6 at $t = 30$ seconds. Fig. 18 shows the nonlinear control surface implemented by the direct adaptive PI fuzzy controller in zone 1 at the end of the experiment (i.e, $t = 60$ seconds). Notice from Fig. 18 how the FMLRC algorithm introduced some significant changes in the control surface if we compare with the fuzzy nonlinear control surface given in Fig. 6.

5. On/off fault tolerance test results

For this experiment, we introduced an on/off fault tolerance test (i.e., where the bulb goes off then later come back on) in single zone and multiple zones scenarios with no partitions between zones. The on/off light bulb failure is five seconds long. We are interested in extensively studying the ability of the FMRLC to reject plant disturbances by learning about the new plant parameters. On the other hand, we are also concerned with comparing both adaptive and nonadaptive control algorithms at the same implementation setting.

5.1. Single zone on/off light bulb failure

The following set of results illustrate the system response for the PI fuzzy controller when an on/off light bulb failure is generated in the experimental testbed at $t = 30$ seconds in zone 1 (i.e., upper left corner). As shown in Fig. 19, at $t = 27.5$ seconds the light bulb failure is initiated in zone 1 and then at $t = 32.5$ seconds the control is given back to the nonadaptive control algorithm. Notice in Fig. 19 that a considerable overshoot peak at approximately 1.75 Volts above the desired light reference level is observed in zone 1 and is propagated to a lesser extent in the other remaining zones as we move away from zone 1. This phenomenon shows the high coupling between the zones due to the maximized cross-illumination effect. In spite of the significant overshoot produced in zone 1 by the on/off failure, the PI fuzzy controller maintains the uniform illumination across the entire smart lights testbed as illustrated in Fig. 19. This behavior again illustrates the disturbance rejection capability of a fuzzy controller.

From Fig. 20 we observe the applied voltage level defined by the nonadaptive control algorithm. In zone 1 it is clear that the on/off failure is introduced between 27.5 and 32.5 seconds of implementation time. Once the control is returned to the controller, the control output is saturated at 10 Volts for few seconds until it is decreased to a steady value. Zone 3 (followed by zone 2) exhibits the highest undershoot peak due to its close proximity to zone 1 (as defined in Fig. 1). Next, implementation results from Fig. 21 show the capability of the adaptive control algorithm to quickly adapt to a significant plant

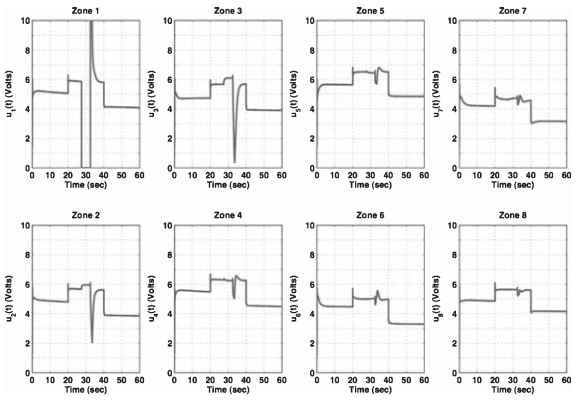

Fig. 20. Applied voltage level to the light bulbs at each zone for the PI fuzzy controller with no partition between zones under zone 1 on/off light bulb failure.

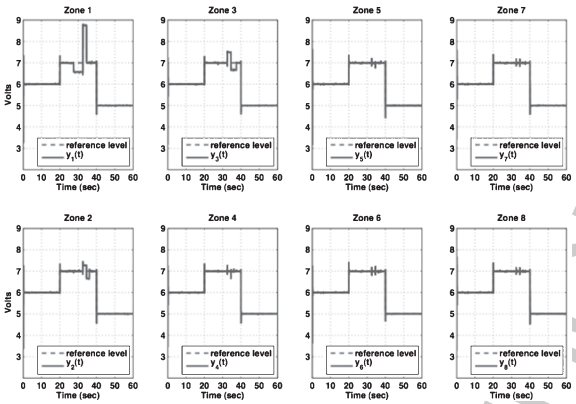

Fig. 21. Light levels at each zone for the direct adaptive PI fuzzy controller with no partition between zones under zone 1 on/off light bulb failure.

disturbance (i.e., the on/off failure). Comparing with the results given in the previous subsection, the adaptive algorithm shows a faster speed of convergence to the desired reference level and smaller overshoots and undershoots as compared to the nonadaptive algorithm. Also, good reference light level tracking is achieved by the adaptive control algorithm.

The applied voltage level defined by the adaptive control algorithm is illustrated in Fig. 22. Observe from Fig. 22 that the adaptive control algorithm does not resemble the same control signal as given by the nonadaptive algorithm (i.e., Fig. 20). Clearly, the learning process forces some significant changes in the control signal as given in zones 2 and 3 respectively which shuts down the light bulbs in these zones until zone 1 controller is able to start tracking the reference light level again.

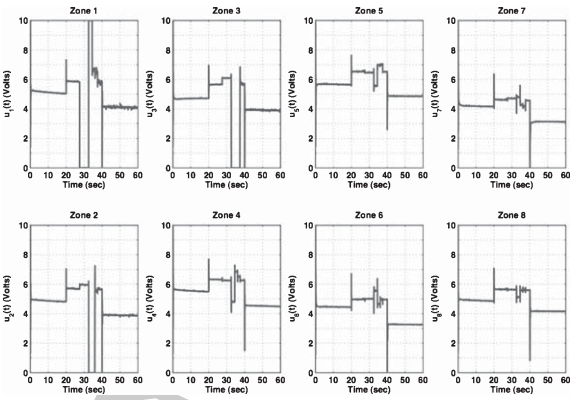

Fig. 22. Applied voltage level to the light bulbs at each zone for the direct adaptive PI fuzzy controller with no partition between zones under zone 1 on/off light bulb failure.

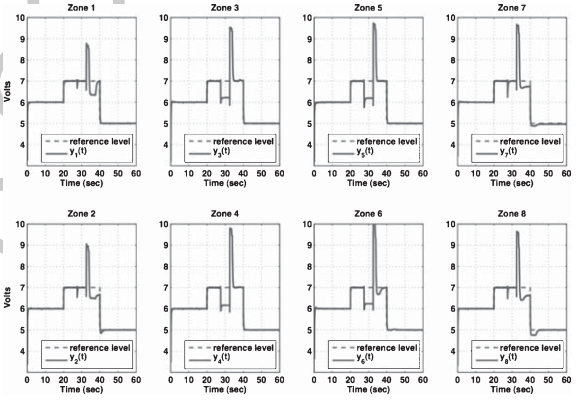

Fig. 23. Light levels at each zone for the PI fuzzy controller with no partition between zones under zones 3, 4, 5 and 6 on/off light bulb failure.

5.2. Multiple zone on/off light bulb failure

Real-time implementations introducing an on/off light bulb failure in multiple zones of the testbed with no partition between zones are investigated next. We generate the on/off failure in the time window between $t = 27.5$ and $t = 32.5$ seconds. Again, we expect that the adaptive control algorithm will outperform the nonadaptive control in all the real-time implementations by means of recovering the desired light reference level in as many of the zones as possible.

An on/off light bulb failure is produced in zones 3, 4, 5, and 6 between $t = 27.5$ and $t = 32.5$ seconds. This implementation scenario represents the case where the plant disturbance due to the on/off failure is maximized. Results prove the poor system performance with the PI fuzzy controller as shown in Fig. 23. Clearly, the

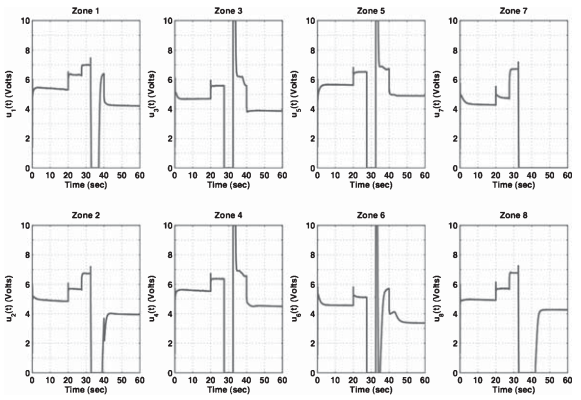

Fig. 24. Applied voltage level to the light bulbs at each zone for the PI fuzzy controller with no partition between zones under zones 3, 4, 5 and 6 on/off light bulb failure.

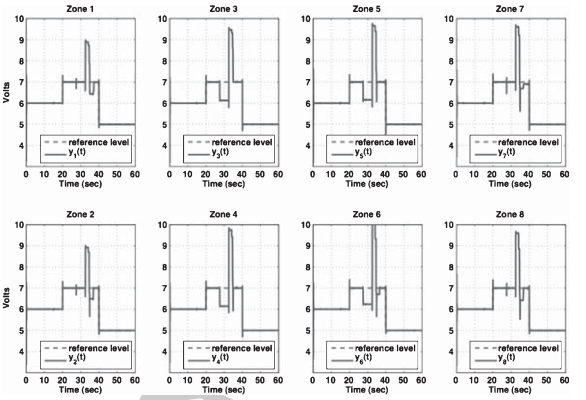

Fig. 25. Light levels at each zone for the direct adaptive PI fuzzy controller with no partition between zones under zones 3, 4, 5 and 6 on/off light bulb failure.

nonadaptive control algorithm fails to maintain the desired reference light level in zones 2, 7 and 8. Actually, only zone 1 (i.e., the only remaining non failing zone) is able to track the reference input only few seconds before the reference input is lowered to 5 Volts. Also, notice in Fig. 23 that zone 7 exhibits a steady state error and zones 2, 7, and 8 present an undershoot after $t = 40$ seconds (i.e., reference input of 5 Volts).

Next, an on/off light bulb failure is created in zones 3, 4, 5, and 6 between $t = 27.5$ and $t = 32.5$ seconds for the adaptive fuzzy controller. Recall that the PI fuzzy controller failed to recover the tracking in zones 2, 7, and 8 between $t = 32.5$ and $t = 40$ seconds (i.e., Fig. 23). From Fig. 25 is apparent that the adaptive fuzzy controller is able to recover the tracking in zones 2 and 6 but there is still a small steady state error (few millivolts) in zone 7. As shown in Fig. 26, the light bulb in zone 7 remains turned off between $t = 32.5$ and $t = 40$ seconds which justifies the presence of the steady state error.

In spite of the inability of the adaptive PI fuzzy controller to regulate zone 7 between $t = 27.5$ and $t = 32.5$ seconds, when the reference input is lowered to 5 Volts at $t = 40$ seconds the adaptive control algorithm is able to track the desired reference light level in all the zones, eliminating the undershoot in zones 2, 7, and 8 and the steady state error in zone 7. Notice from Fig. 26 that the adaptive algorithm can maintain all the light bulbs turned on immediately after the last reference input is introduced at $t = 40$ seconds.

In Fig. 18, we illustrated the ability of the FMRLC to adapt the nonlinear control surface during a multiple zone light bulb failure. Again, it is desirable to emphasize the learning capacity of the FMRLC by

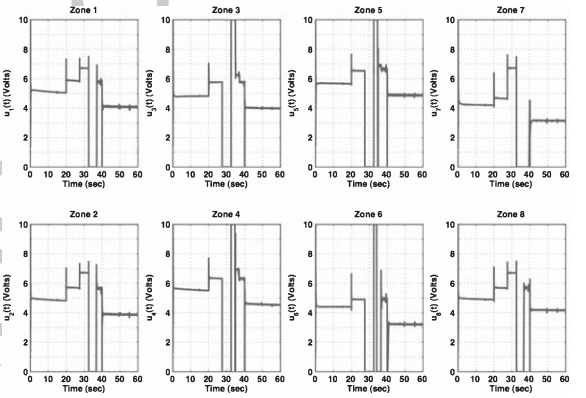

Fig. 26. Applied voltage level to the light bulbs at each zone for the direct adaptive PI fuzzy controller with no partition between zones under zones 3, 4, 5 and 6 on/off light bulb failure.

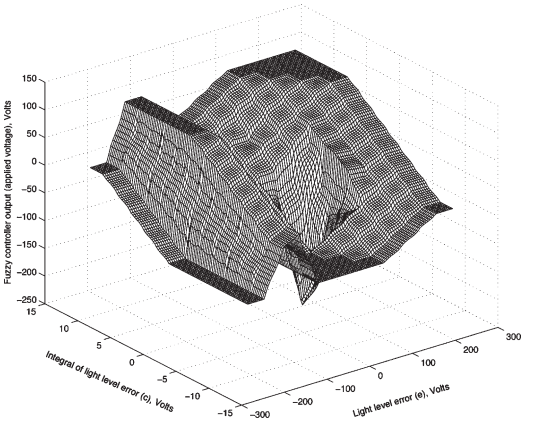

Fig. 27. Nonlinear control surface implemented by the direct adaptive PI fuzzy controller in zone 1 at $t = 35$ seconds under an on/off light bulb failure in zones 3, 4, 5 and 6.

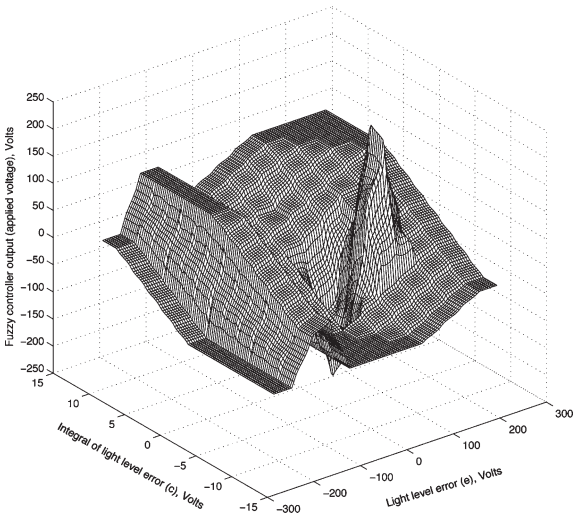

Fig. 28. Nonlinear control surface implemented by the direct adaptive PI fuzzy controller in zone 1 at $t = 60$ seconds under an on/off light bulb failure in zones 3, 4, 5 and 6.

presenting the nonlinear control surface achieved when an on/off light bulb failure is introduced in zones 3, 4, 5, and 6 between $t = 27.5$ and $t = 32.5$ seconds. Notice from Fig. 27 how the FMRLC quickly adapts the nonlinear control surface compared to the multiple zone light bulb failure case given in Fig. 18. Moreover, observe from Fig. 28 how the FMRLC kept adapting the control surface by the end of the experiment (i.e., $t = 60$ seconds). This clearly proves the benefits of having an adaptive control algorithm in order to obtain a satisfactory performance under several scenarios.

6. Sensor failure test results

The sensor failure test provides the situation where the illumination is maximized (i.e., light bulb is turned on at maximum applied voltage) in the zone when the failure occurs and an over-illumination unbalance is introduced to the testbed via the cross-illumination between zones. This test is performed for half-height partitions between zones in order to attenuate the cross-illumination effect so that the impact of the sensor failure can be analyzed and compensated by the fuzzy controller.

6.1. Two-zone sensor failure

Sensor failures are generated in zones 3 and 6 at $t =$ 30 seconds. For this sensor failure case, the PI fuzzy

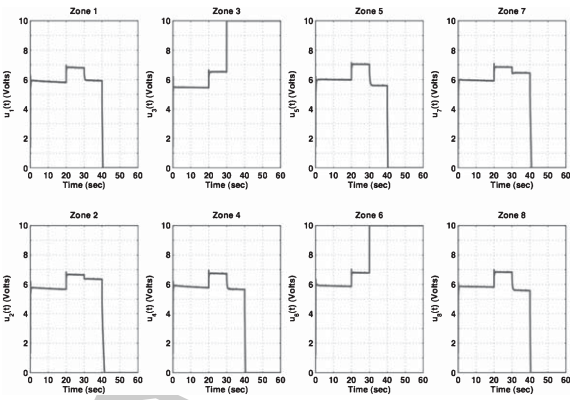

Fig. 29. Light levels at each zone for the PI fuzzy controller with half partition between zones under zones 3 and 6 sensor failure.

controller is able to track the desired reference lighting level in zones 1, 2, 4, 5, 7, and 8 until $t = 40$ seconds as shown in Fig. 29. Once the reference input is lowered to 5 Volts, the fuzzy controller cannot track the voltage reference input in all the remaining controlled zones because each controlled zone is a neighboring zone of a failing zone. From Fig. 29 it is evident how the voltage level in the uncontrolled zones (i.e., zones 3 and 6) drops to a fixed constant value. Evidently, each failing zone has more than two neighboring zones which supports the fact that the fuzzy controller is unable to keep the uniform lighting after $t = 40$ seconds.

When the sensor failure occurs in zones 3 and 6 at $t = 30$ seconds, the failure is given by a clamp at 10 Volts of the applied voltage in the corresponding failing zones as illustrated in Fig. 30. Following the sensor failures, the remaining controlled zones react to the sensor

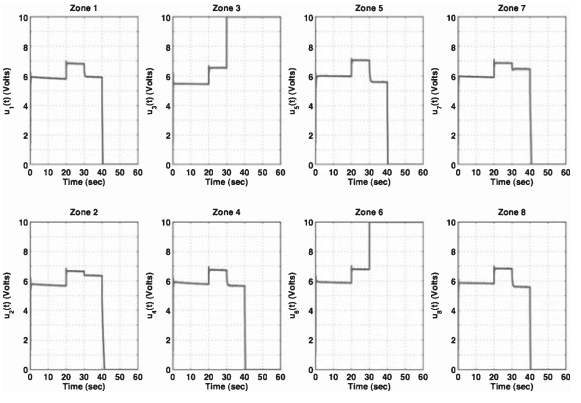

Fig. 30. Applied voltage level to the light bulbs at each zone for the PI fuzzy controller with half partition between zones under zones 3 and 6 sensor failure.

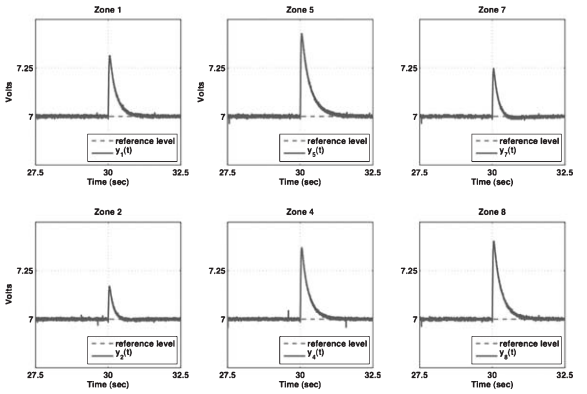

Fig. 31. Light level in controlled zones 1, 2, 4, 5, 7, and 8 for the PI fuzzy controller with half partition between zones under zones 3 and 6 sensor failure.

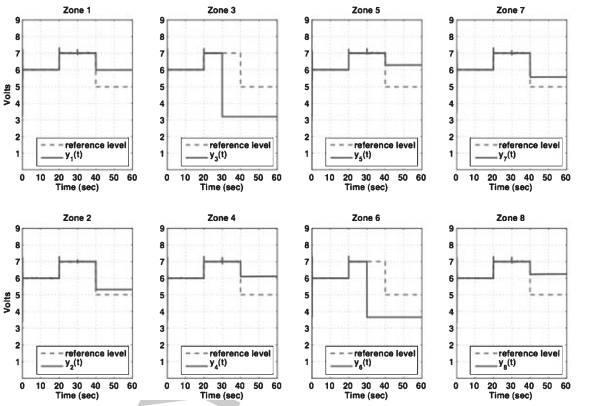

Fig. 32. Light levels at each zone for the direct adaptive PI fuzzy controller with half partition between zones under zones 3 and 6 sensor failure.

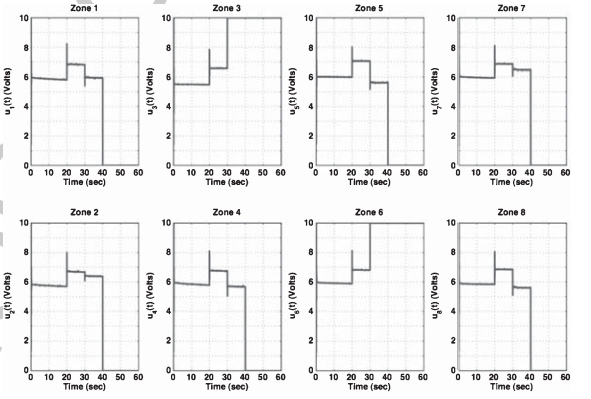

Fig. 33. Applied voltage level to the light bulbs at each zone for the direct adaptive PI fuzzy controller with half partition between zones under zones 3 and 6 sensor failure.

failure by immediately decreasing their corresponding applied voltage level in order to maintain uniform lighting. Thus, an overshoot is generated in each controlled zone (as given in Fig. 29) and it is related to the increased cross-illumination effect that was generated by the maximum illumination (i.e., applied voltage clamp at 10 Volts) produced in the sensor failing zones 3 and 6 as shown in Fig. 30. After $t = 40$ seconds, all the light bulbs in the remaining controlled zones (i.e., zones 1, 2, 4, 5, 7, and 8) are turned off and the fuzzy controller is unable to keep track of the desired voltage reference input.

A detailed view of the light level in the controlled zones (i.e., zones 1, 2, 4, 5, 7 and 8) in a $t = 27.5$ to $t = 32.5$ seconds window is shown in Fig. 31. Zone 5 has the highest overshoot peak at approximately 0.40 Volts above the reference voltage and zone 2 has the smallest overshoot peak at approximately 0.13 Volts above the reference voltage. In addition, zone 5 has the longest settling time of approximately 1.2 seconds and zone 2 has the shortest settling time of approximately 0.5 seconds. Clearly, zone 5 is most affected zone by the increased cross-illumination effect that was generated by the maximum illumination (i.e., applied voltage clamp at 10 Volts) produced in zones 3 and 6 where the sensors fail, and following in decreasing order zones 8, 4, 1, 7 and 2. Since the zones in the testbed are not symmetrically distributed (see Fig. 1), the behavior given in Fig. 31 is expected.

Next, sensor failures are generated in zones 3 and 6 at $t = 30$ seconds for the adaptive control algorithm. For this case, where the failing zones are also neighboring zones, the adaptive controller is able to maintain the uniform illumination in the tested in the controlled zones 1, 2, 4, 5, 7 and 8 until $t = 40$ seconds as presented in Fig. 32. Evidently, there is a clear decrease in the overshoot and undershoot peaks for those zones closer to the failing zones compared with the nonadaptive controller (i.e., see Fig. 29).

Notice from Fig. 32 that the uncontrolled zones present the same fixed light level between $t = 30$ and $t = 60$ seconds due to the sensor failures. After $t = 40$ seconds, all the remaining controlled zones exhibit different fixed light levels above the desired voltage reference input which are defined by the cross-illumination effect created by the maximum illumination (i.e., applied voltage clamp at 10 Volts) produced in the failing zones 3 and 6 as illustrated in Fig. 33. The applied voltage level given by the adaptive controller in Fig. 33 is similar to the performance described by the

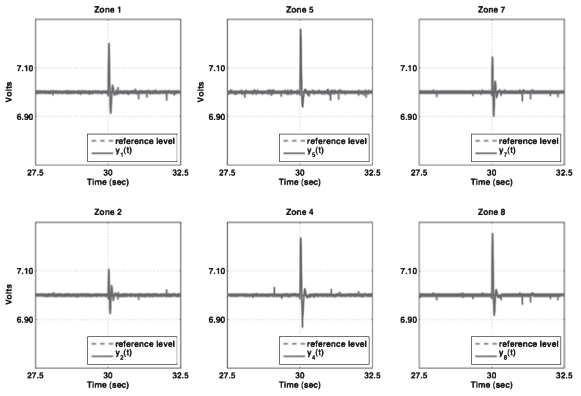

Fig. 34. Light level in controlled zones 1, 2, 4, 5, 7, and 8 for the direct adaptive PI fuzzy controller with half partition between zones under zones 3 and 6 sensor failure.

nonadaptive controller in Fig. 30 but again characterized by a faster rejection of the sensor failure.

Looking at Fig. 34, the highest overshoot peak is given by zone 5 at approximately 0.25 Volts above the desired voltage reference level which is a 37.5% peak reduction compared to the nonadaptive controller (i.e., Fig. 31). The highest undershoot peak is shown by zone 4 at 0.15 Volts below the desired voltage reference level. In addition, a faster settling time of approximately 0.15 seconds is achieved in all the controlled zones which represents a 87.5% reduction in settling time compared with the worst case (i.e., $t_s = 1.2$ seconds) for the nonadaptive controller.

7. Conclusion

In this paper, we have been able to demonstrate the potential of fuzzy control over other conventional methods for our smart lighting system in achieving uniform illumination across the testbed despite plant variations (i.e., changes in the partition settings), single zone and multiple zones light bulb failures, and two-zone sensor on/off failures. Based on the implementation results presented in this paper, we have proven the benefits of the fuzzy model reference learning controller algorithm for controlling our smart light experimental testbed. The FMRLC has great potential as a smart light control algorithm for the following reasons: a detailed mathematical model of the plant to be controlled is not necessary, the learning mechanism provides an automatic way to adjust the fuzzy control rule-base to make the closed-loop system behave like a desired reference model, and the adaptation mechanism provides rejection of the effect of parameter variations and/or disturbances which results in a more "robust" controller compared to the (nonadaptive) fuzzy controller. As a future direction, it would be of interest to determine if other adaptive fuzzy/neural controllers can achieve high performance as fault tolerant controllers for smart lights. Some of the first methods to consider would be those in [17] and [18]. Also, it would be quite useful to consider (i) experimental testbeds with a larger scale, and different structure (e.g., mixes of partitions and larger open areas); and (ii) a commercial application for a whole floor of a building, or indeed a whole building. In all these contexts, it would be useful to consider changes in external lighting due to the sun and clouds, that impacts lighting in buildings via windows, and how it impacts the control of the lighting levels and lighting uniformity. It would also be important, for a real application in a building, to assess the level of energy savings that can be gained via lighting controls.

References

[1] Y. Diao and K.M. Passino, Fault tolerant stable adaptive fuzzy/neural control for a turbine engine, *IEEE Transactions on Control Systems Technology* **9**(3) (2001), 494–509.

[2] Y. Diao and K.M. Passino, Intelligent fault tolerant control using adaptive and learning methods, *Control Engineering Practice* **10**(8) (2002), 801–817.

[3] Y. Diao and K.M. Passino, Stable adaptive control of feedback linearizable time-varying nonlinear systems with application to fault tolerant engine control, *International Journal of Control* **77**(17) (2004), 1463–1480.

[4] R.F. Hughes and S.S. Dhannu, Substantial Energy Savings through Adaptive Lighting, *2008 IEEE Electrical Power & Energy Conference*, 2008, pp. 1–4.

[5] M.T. Koroglu and K.M. Passino, The illumination balancing algorithm for smart lights, *IEEE Transactions on Control Systems Technology* **22**(2) (2014), 557–567.

[6] W.A. Kwong, K.M. Passino, E.G. Lauknonen and S. Yurkovich, Expert Supervision of Fuzzy Learning Systems for Fault Tolerant Aircraft Control, *Special Issue on Fuzzy Logic in Engineering Applications, Proceedings of the IEEE*, **83**(3) (1995), 466–483.

[7] J.R. Layne and K.M. Passino,. Fuzzy model reference learning control, *Journal of Intelligent and Fuzzy Systems* **4**(1) (1996), 33–47.

[8] J.R. Layne and K.M. Passino, Fuzzy model reference learning control for cargo ship steering, *IEEE Control Systems Magazine* **13**(6) (1993), 23–34.

[9] L. Martirano, A Smart Lighting Control to Save Energy, *The 6th IEEE International Conference on Intelligent Data Acquisition and Advanced Computing Systems: Technology and Applications* **1** (2011), 132–138.

[10] E. Mills, Global lighting energy savings potential, *Light and Engineering* **10** (2002), 5–10.

[11] R. Ordóñez and K.M. Passino, Stable multiple-input multiple-output adaptive fuzzy/neural control, *IEEE Transactions on Fuzzy Systems* **7**(3) (1999), 345–353.

[12] K.M. Passino, *Biomimicry for Optimization, Control, and Automation*. Springer-Verlag, London, UK, 2005.
[13] K.M. Passino and S. Yurkovich, *Fuzzy Control*. Addison-Wesley-Longman, Menlo Park, CA, 1998.
[14] S.S. Phadke, Distributed Control for Smart Lights. Master's thesis. The Ohio State University, 2010.
[15] K.M. Schultz, Distributed Agreement: Swarm Guidance to Cooperative Lighting. PhD dissertation, The Ohio State University, 2010.
[16] Silonex. CdS Photocell. http://www.farnell.com/datasheets/491819.pdf. Online; accessed 19-March-2012.
[17] J.T. Spooner and K.M. Passino, Stable adaptive control using fuzzy systems and neural networks, *IEEE Transactions on Fuzzy Systems* **4**(3) (1996), 339–359.
[18] J.T. Spooner, M. Maggiore, R. Ordóñez and K.M. Passino, *Stable Adaptive Control and Estimation for Nonlinear Systems: Neural and Fuzzy Approximator Techniques*. JohnWiley and Sons, NY, 2002.
[19] ENERGY STAR, the U.S. Environmental Protection Agency, and the U.S. Department of Energy. Lighting for Building and Plants. http://www.energystar.gov/buildings?s=mega. Online; accessed 12/20/14.
[20] Y.-J. Wen and A.M. Agogino, Wireless Networked Lighting Systems for Optimizing Energy Savings and User Satisfaction, *Proceedings of the 2008 IEEE Wireless Hive Networks Conference*, 2008.
[21] Y.-J. Wen, J. Bonnell and A.M. Agogino, Energy Conservation Utilizing Wireless Dimmable Lighting Control in a Shared-Space Office, *Proceedings of the 2008 Annual Conference of the Illuminating Engineering Society*, 2008.